https://doi.org/10.7840/kics.2024.49.12.1739

Digital Precoder-Combiner and Power Allocation Optimization in MU MIMO-NOMA: A Quantum Neural Network Approach

Lia Suci Waliani•, Soo Young Shin°

ABSTRACT

This paper proposes a quantum neural network (QNN) to address joint optimization in wireless communication. By utilizing the advantages of quantum entanglement and superposition in quantum computing and machine learning, QNN can solve optimization problems with lower complexity than classical neural networks, due to its parallel processing capabilities. Specifically, this study applies QNN to jointly optimize digital precoder-combiner and power allocation in a multi-user multiple-input multiple-output non-orthogonal multiple access (MU MIMO-NOMA) system. The performance of the QNN is analyzed and presented.

Key Words : digital precoding, digital combiner, quantum neural network, wireless optimization

Ⅰ. Introduction

The rapid advancement of wireless communication technology has led to a demand for higher data rates, particularly as we move towards the implementation and deployment of beyond 5G (B5G) and 6G networks[1-3]. This surge in demand is driven by the growing need for faster, more reliable, and more efficient communication capabilities to support an ever-increasing number of connected devices and data-intensive applications. Multipleinput multiple-output (MIMO) technology, which leverages the use of multiple antennas at both the transmitter and receiver ends, has emerged as a highly promising and effective solution to meet this demand[4,5]. By enabling simultaneous transmission and reception of multiple data streams, MIMO technology significantly enhances spectral efficiency and overall network performance, making it an essential component in the evolution of wireless communication systems.

The concept of MIMO is often enhanced by the use of beamforming. Beamforming is a signal processing technique used in wireless communication systems to direct the transmission or reception of signals in specific directions[6]. In beamforming architectures, both analog and hybrid beamforming use phase shifters, which can cause quantization errors because of their limited resolution and non-linear properties. These errors can negatively impact the system's overall performance[7]. Fully digital precoding, on the other hand, offers greater flexibility in beam steering by allowing baseband processors to directly generate phase and magnitude values for each channel, resulting in higher resolution and improved spectral efficiency[8].

Given the potential for a higher number of users

※ This research was supported by the MSIT(Ministry of Science and ICT), Korea, under the ITRC(Information Technology Research Center) sup- port program(IITP-2024-RS-2024-00437190) supervised by the IITP(Institute for Information & Communications Technology Planning & Evaluation). This work was supported by Institute of Information & communications Technology Planning & Evaluation (IITP) grant funded by the Korea govern- ment(MSIT) (No. 2021-0-02120, Research on Integration of Federated and Transfer learning between 6G base stations exploiting Quantum Neural Networks).

• First Author : Kumoh National Institute of Technology, Department of IT Convergence Engineering; liasuciwaliani@kumoh.ac.kr, 학생회원

° Corresponding Author : Kumoh National Institute of Technology, Department of IT Convergence Engineering; wdragon@kumoh.ac.kr, 종신회원

논문번호 : 202405-107-B-RE, Received May 21, 2024; Revised July 3, 2024; Accepted Augst 27, 2024

compared to transmit antenna elements, integrating nonorthogonal multiple access (NOMA) with MIMO systems can further enhance spectral efficiency[9]. Achieving maximum spectral efficiency necessitates the joint optimization of transmit precoding, receiver combining, and NOMA power allocation. However, this optimization problem is non-convex and computationally intensive due to the high dimensionality of the variables involved. Conventional methods, such as mathematical derivation[10] and the iterative algorithm[11] often struggle to find optimal solutions efficiently. In order to address this issue, classical machine learning techniques can tackle non-convex optimization problems[12].

However, the complexity of classical machine learning algorithms tends to grow significantly as the amount of data being processed increases. This escalation in complexity often leads to longer computation times and greater demand for computational resources. This is primarily due to the serial processing nature of neurons in classical computers. To address this issue, quantum machine learning has emerged as a promising solution[13]. The advantages of quantum computing, such as parallel processing, lead to lower complexity and reduced processing times. By leveraging the principles of quantum computing and machine learning, quantum machine learning can potentially reduce computational complexity and improve processing speeds, offering a more efficient and scalable approach to solving complex problems. The inherent advantages of quantum computing to tackle complex optimization problems, provide a robust framework for enhancing the efficiency and effectiveness of these critical tasks[14,15].

To the best of the authors' knowledge, the utilization of QNN for joint optimization for both digital precodercombiner and resource allocation is still limited. Accordingly, the contribution of this study proposes the use of a quantum neural network (QNN) for the joint optimization of digital precoder-combiner and resource allocation in multi-user multiple-input multiple-output nonorthogonal multiple access (MU MIMO-NOMA) systems.

The structure of this paper is as follows. Section II presents the wireless system models for digital precodercombiner and NOMA power allocation. Section III describes the proposed quantum neural network (QNN) approach. Section IV discusses and analyzes the performance of the proposed QNN. Finally, the conclusions are drawn in Section V.

Notations: Transpose and conjugate transpose are denoted by $(\cdot)^T$ and $(\cdot)^H$, respectively. $(\cdot)^{-1}$ indicates inversion. $\otimes$ indicates Kronecker product. Normal and circular normal distributions are presented as $\mathcal{N}(\mu, \sigma^2)$ and $\mathcal{CN}(\mu, \sigma^2)$, respectively, where μ is the mean and σ^2 is the variance. $|\cdot|$ and $\|\cdot\|$ are indicating the absolute and norm values, respectively.

Ⅱ. Wireless System Model

This study is concerned with a single base station (BS) serving multiple users (UEs) that are grouped in NOMA groups. Subsequently, this study assumes that each group consists of two users. The BS employs a downlink communication MU MIMO-NOMA system. The received signal $\mathbf{y}_{k,m}$ at the k-th UE and m-th group can be expressed as

$$\mathbf{y}_{k,m} = \underbrace{\sqrt{\mathbf{g}_{k,m}}\mathbf{c}_{k,m}\mathbf{H}_{k,m}^{H}\mathbf{v}_{k,m}\mathbf{x}}_{\text{desired signal}} + \underbrace{\sum_{i=1,i\neq k}^{K}\sqrt{\mathbf{g}_{i,m}}\mathbf{c}_{i,m}\mathbf{H}_{k,m}^{H}\mathbf{v}_{i,m}\mathbf{x}}_{\text{interference signal}} + \underbrace{\mathbf{n}_{k,m}}_{\text{noise}}, \quad (1)$$

where $\mathbf{H}_{k,m} \in \mathbb{C}^{S_{\text{Tx}} \times N_{\text{rx}}}$, $\mathbf{c}_{k,m}$, $\mathbf{v}_{k,m}$, $n_{k,m}$ denote the channel matrix information, digital precoding, receiver combiner, transmitted data stream, additive white Gaussian noise (AWGN) denoted as $\mathcal{CN}(0, \sigma^2)$ at NRx receive antenna of each user, respectively.

In order to serve multiple UEs, the BS employs a uniform planar antenna (UPA) with dimensions $S_{\text{Tx}} = M_{\text{Tx}} \times N_{\text{Tx}}$, consisting of two-dimensional antenna elements. Conversely, each receiving UE utilizes a uniform linear antenna (ULA) with NRx one-dimensional array antenna elements. Thus, the downlink channel matrix for the k-th UE at m-th group can be expressed as

$$\mathbf{H}_{k,m} = \sqrt{\frac{S_{\mathrm{Tx}} N_{\mathrm{Rx}}}{U_{\mathrm{path}}}} \sum_{u=1}^{U_{\mathrm{path}}} \psi_{k,u} \mathbf{a}_{k,r}(\theta_{k,u}^{r}) \mathbf{a}_{k,t}^{H}(\theta_{k,u}^{t}, \phi_{k,u}^{t}), \tag{2}$$

where $\psi_{k,l} \sim \mathcal{CN}(0, 1)$, $\mathbf{a}_{k,r}$, and $\mathbf{a}_{k,t}$ denotes a complex gain of u-th path, ULA array response vector, and UPA array response vector, respectively. The array response vector of ULA antennas can be expressed as

$$\mathbf{a}_{k,r}(\theta_{k,u}^{r}) = \frac{1}{\sqrt{N_{\mathrm{Tx}}}} \left[1, e^{j\omega\cos(\theta_l^r)}, \ldots, e^{j\omega(N_1)\cos(\theta_u^r)}\right]^{\mathrm{T}}, \tag{3}$$

where $\omega = \frac{2\pi d}{\lambda}$ λ, the λ denotes the wavelength, d denotes the distance between two antennas which can be defined as $d = \frac{\lambda}{2}$, and $\theta_{k,u}^{r} \in [0, 2\pi]$ is the elevation angle of arrival (AoA). For a UPA the array response vector can be expressed as

$$\mathbf{a}_{k,t}(\theta,\phi)_{k,u}^{t} = \frac{1}{\sqrt{S_{\mathrm{Tx}}}} \left[1, e^{j\omega\sin(\theta_u^t)[(m-1)\cos(\phi_u^t)+(n-1)\sin(\phi_u^t)}, \ldots, e^{j\omega\sin(\theta_u^t)\left[(M-1)\cos(\phi_u^t)+(N-1)\sin(\phi_u^t)\right]}\right]^{\mathrm{T}}, \tag{4}$$

where $(\theta_{k,l}^{t}, \phi_{k,l}^{t}) \in [0, 2\pi]$ denotes the elevation and azimuth angles of departure (AoD).

2.1 Digital Precoder

As illustrated in Fig. 1, the transmitter BS generates digital precoding vectors to serve multiple UEs. Digital precoding is employed to enhance signal quality by directing the signal to the intended UEs. Let $\mathbf{v}_{k,m}$ be the precoding vectors for the k-th UE at the m-th group. According to [16], the digital precoding can be expressed as

$$\mathbf{v}_{k,m} = \sqrt{\mathbf{g}_{k,m}} \frac{\left(\mathbf{I}_K + \frac{1}{\sigma^2}\sum_{k=1}^{K} \xi_{k,m}\mathbf{H}_{k,m}\mathbf{H}_{k,m}^{H}\right)^{-1}\mathbf{H}_{k,m}}{\left\|\mathbf{I}_K + \frac{1}{\sigma^2}\sum_{k=1}^{K} \xi_{k,m}\mathbf{H}_{k,m}\mathbf{H}_{k,m}^{H}\right)^{-1}\mathbf{H}_{k,m}\right\|}, \tag{5}$$

where $\mathbf{I}_K$ denotes the identity matrix with $K \times K$ dimension, $\mathbf{H}_{k,m}$ denotes the channel matrix for k-th UE at the m-th group, and $\xi_{k,m}$ denotes the optimization variable that can be obtained from QNN.

2.2 Digital Combiner

On the other hand, at the receiver, the received signal undergoes processing, where a digital combiner incorporating an RF chain is employed to integrate and process the incoming signals. Let $\mu_{k,m}$ be the optimization variable that can be obtained from the QNN, thus the optimal combiner $\mathbf{c}_{k,m}$ for the k-th user at the m-th group can be expressed as [17]

$$\mathbf{c}_{k,m} = \mu_{k,m}\left(\left(\mathbf{H}_{k,m}^{H}\mathbf{H}_{k,m} + \gamma_{k,m}^{-1}I\right)^{-1}\mathbf{H}_{k,m}^{H}\right). \tag{6}$$

2.3 NOMA Power Allocation

Let us assume channel gains of the users in a NOMA group are sorted in descending order as follows $|\mathbf{H}_1|^2 \geq \cdots \geq |\mathbf{H}_K|^2$. Successive interference cancellation (SIC) is applied at the receivers for multi-user detection and decoding to mitigate inter-user

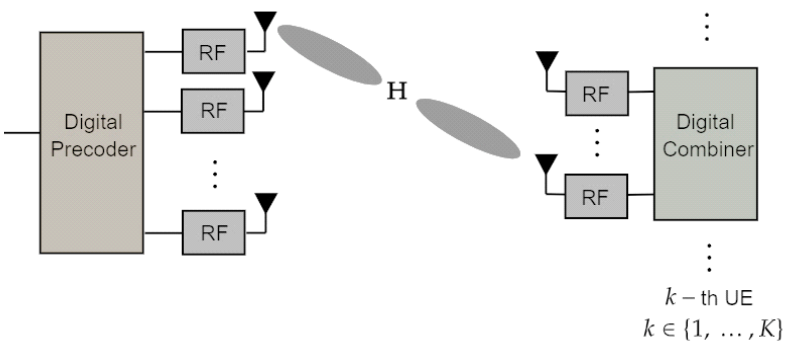

Fig. 1. A digital precoder-combiner structure in MU MIMO-NOMA.

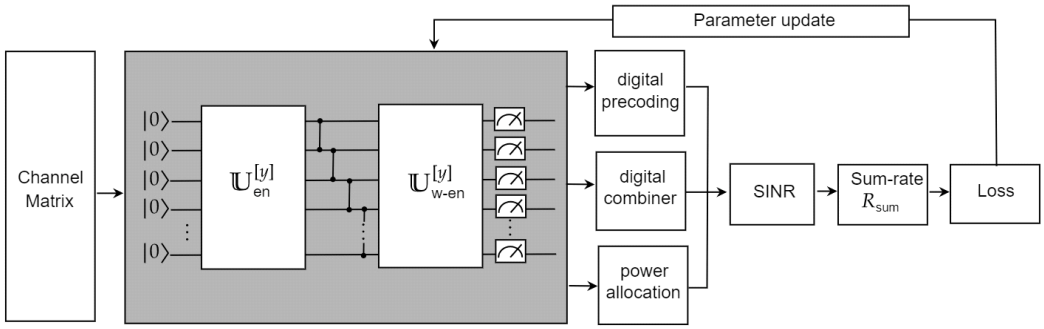

Fig. 2. The scheme of the proposed QNN.

interference. The received signal-to-interference-plus-noise ratio (SINR) can be calculated as follows

$$\Upsilon_{k,m} = \frac{\mathbf{g}_{k,m}|\mathbf{c}_{k,m}\mathbf{H}_{k,m}^{H}\mathbf{v}_{k,m}|^2}{\sum_{i=k+1}^{K}\mathbf{g}_{i,m}|\mathbf{c}_{k,m}\mathbf{H}_{k,m}^{H}\mathbf{v}_{i,m}|^2+\sigma^2}, \tag{7}$$

where the σ^2 indicates the noise variance.

The power allocation for the k-th user in the m-th group can be calculated as $\mathbf{g}_{k,m} = \lambda_{k,m}G_{\text{tot}}$, where $\lambda_{k,m} \in [0, 1]$ is the NOMA power coefficient and G_{tot} is the total power in the transmitting BS. The achievable rate for the k-th user at the m-th group can be expressed as follows

$$R_{\text{sum}} = \frac{B}{M}\sum_{m=1}^{M}\sum_{k=1}^{K}\log_2(1+\Upsilon_{k,m}), \tag{8}$$

where B is the bandwidth and M denotes the number of grouping.

2.4 Problem Formulation

The objective function is to maximize the achievable sum rate given precoder, combiner, and power allocation in MU MIMO-NOMA which can be formulated as follows:

$$\max_{\mathbf{v},\mathbf{c},\mathbf{g}} \quad R_{\text{sum}} = \frac{B}{M}\sum_{m=1}^{M}\sum_{k=1}^{K}\log_2(1+\Upsilon_{k,m}) \tag{9a}$$

$$\text{s.t.} \quad C_1 : R_{\text{sum}} \geq R_{\min}, \tag{9b}$$

$$C_2 : ||c_{k,m}||^2 \leq 1, \forall k \in \{1,\ldots,K\}, \tag{9c}$$

$$C_3 : 0 < \sum_{k=1}^{K}\lambda_{k,m} \leq 1. \tag{9d}$$

Ⅲ. Quantum Neural Network for Precoder-Combiner and Power Allocation

This section presents the proposed QNN. The proposed QNN network consists of one layer employed to obtain optimization variables. The quantum circuit of QNN is designed and presented in Fig. 2. Herein, inputs of the network in classical values are mapped into quantum states as qubits through the encoding process. In this case, the number of qubits denoted as N_{qubits}, possesses an identical dimension with the network inputs, thus $N_{\text{qubits}} = N_{\text{inputs}}$. As an initial step, each qubit is placed into a quantum superposition state using a Hadamard operator which is defined as pre-processing, expressed as

$$\mathbb{U}_{\text{pre-processing}} \triangleq \bigotimes_{n=1}^{N_{\text{inputs}}}\mathbf{H}(|u_n\rangle). \tag{10}$$

Subsequently, the pre-processed qubits are going through a feed-forward process. The feed-forward process begins with data encoding, where the classical input is mapped onto the quantum states of qubits. The unitary for input data in the y-th layer can be expressed as

$$\mathbb{U}_{\text{w-en}}^{[y]} = \bigotimes_{n=1}^{N_{\text{qubit}}}\mathbf{RX}(\tanh(w_n)), \tag{11}$$

where $\mathbf{RY}(\bullet)$ denotes the quantum gates for rotating qubits around the Y–axis of the *Bloch sphere*[1] within

1) Bloch sphere is a geometrical representation of the

θ phase. Afterward, identical to data encoding, weight encoding is also mapped onto the quantum states. The unitary function of weight encoding in the y-th layer can be expressed as

$$\mathbb{U}_{\text{w-en}}^{[y]} = \bigotimes_{n=1}^{N_{\text{qubit}}} \mathbf{RX}(\tanh(w_n)), \tag{12}$$

where $\mathbf{RX}(\bullet)$ denotes the quantum gates for rotating qubits around the X−axis by θ phase. Subsequently, a feed-forward process of QNN denoted by $\mathbb{U}_{\text{QNN}}$, can be expressed as

$$\begin{aligned}\mathbb{U}_{\text{QNN}} \triangleq & \bigotimes_{n=1}^{N_{\text{input}}} \mathbf{RX}\Big(\tanh\left[w_n\right]\Big) \\ & \prod_{n=1}^{N_{\text{input}}} \mathbf{CZ}\Big(|\mathbf{u}_n\rangle \,\Big|\, |\mathbf{u}_{n-1}\rangle\Big) \otimes \ldots \otimes \\ & \mathbf{CZ}\Big(|\mathbf{u}_{N_{\text{input}}}\rangle \,\Big|\, |\mathbf{u}_{N_{\text{input}}-1}\rangle\Big) \otimes \\ & \mathbf{RY}\Big(\tanh\left[\mathbf{u}_n\right]\Big),\end{aligned} \tag{13}$$

where w_n denotes the trainable weights for the n-th qubit, $\mathbf{u}_n$ denotes the classical input for the n-th qubit, and $\mathbf{CZ}(\cdot)$ denotes an operation of connecting two qubits.

Considering the loss value is obtained as a classical value, a quantum measurement is performed at the end of the total layers to obtain outputs in real values. The quantum measurement operation, denoted by $\mathbf{M}_{\text{QNN}}^{(y)}$, can be expressed as

$$\mathbf{M}_{\text{QNN}}^{(y)} = \langle 0|\, \mathbb{U}_{\text{QNN}}(w)^{\dagger} \mathbf{H} \mathbb{U}_{\text{QNN}}(w)\, |0\rangle. \tag{14}$$

In order to mitigate the inherent perturbations present within quantum measurement processes because of the noise, the measurement is conducted for y_{shot} times. Therefore, the measurement outputs can be expressed as

$$y = \frac{1}{y_{\text{shot}}} \sum_{y=1}^{y_{\text{shot}}} \mathbb{M}_{\text{QNN}}^{(y)}. \tag{15}$$

quantum bits (qubits).

Based on the outputs, the loss of QNN can be calculated as follows

$$\mathbf{L}_{\text{QNN}}(w) = -\frac{1}{N_{\text{data}}} \sum_{n=1}^{N_{\text{data}}} \Xi(y)_n, \tag{16}$$

where N_{data} denotes number of training data in a batch, while $\Xi(y)$ denotes an objective output. Subsequently, a gradient of the QNN can be calculated using parameter-shift rules[18] as follows

$$\nabla \mathbf{L}_{\text{QNN}}(w) = \frac{\mathbf{L}_{\text{QNN}}(w+\theta) - \mathbf{L}_{\text{QNN}}(w-\theta)}{2\sinh(\theta)}, \tag{17}$$

where $\theta \in [0, \pi]$ denotes a shifting parameter. Finally, the trainable weights can be updated as follows

$$w' = w - \alpha \nabla \mathbf{L}_{\text{QNN}}(w), \tag{18}$$

where $\alpha \in (0, 1]$ denotes the learning rate.

3.1 QNN for MU MIMO-NOMA Optimization

The details for solving the joint optimization problem in the MU MIMO-NOMA scenario can be described as follows:

1. The inputs for the QNN are the channel matrices for each UE, as described in Eq. (2). The total number of elements in the channel matrix is equal to the total number of inputs in the QNN network.
2. The problem formulation has been presented in Section II, where the optimized variables become the output of the QNN. Specifically, the optimization variables $\xi_{k,m}$, $\mu_{k,m}$, and $\lambda_{k,m}$ denote the precoders, combiner, and power allocation, respectively.

Ⅳ. Numerical Result

This section analyses the performance of QNN for digital precoder-combiner optimization. The simulation parameters are given in Table 1. It is worth noting that quantum computers are still in the early stages of development, and the number of qubits

Table 1. Parameters

Parameters	Values
N_{user}	4
N_{Tx}	2
M_{Tx}	2
$S_{\text{Tx}} = N_{\text{Tx}} \times M_{\text{Tx}}$	4
N_{Rx}	2
B	8.64 MHz
N_{data}	50
N_{test}	1000
y_{shot}	1024
α	0.01

available for use is currently limited. Therefore, this study considers the low number of the antenna and users. The quantum unitary UQNN was executed utilizing a "basic simulator" backend in IBM Qiskit[19].

4.1 Loss

The training loss with respect to the number of training episodes was presented in Fig. 3. In this study, unsupervised learning was employed, which contrasted with supervised learning, unsupervised learning performed the optimization task without needing reference data. Therefore, the loss function can be expressed as $\mathbf{L}\text{QNN} = -\frac{1}{N_{\text{data}}}\sum_{n=1}^{N_{\text{data}}} R_{\text{sum}}$. As can be seen, the loss function showed a decreasing trend starting from the first training episode. Furthermore, the loss is converged at 3-th training episode.

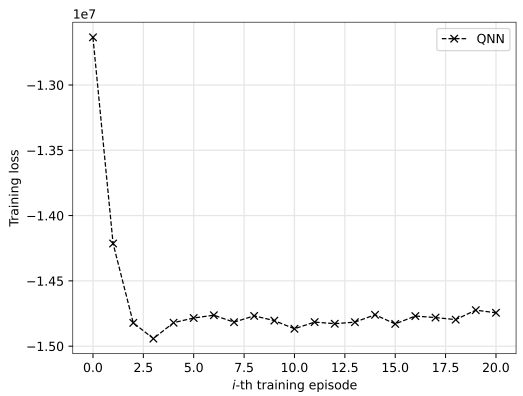

Fig. 3. The training loss.

4.2 Achievable Sumrate

The achievable rate with respect to the transmitted SNR in MU MIMO-NOMA is presented in Fig. 4 . As shown, the achievable sum rate for QNN optimization has improved compared to the unoptimized scheme. In the unoptimized scheme, all the optimization coefficients are set to 1, meaning there is no optimization for the precoder and combiner. Additionally, the power allocation coefficient is set to 0.2 for near users and 0.8 for far users.

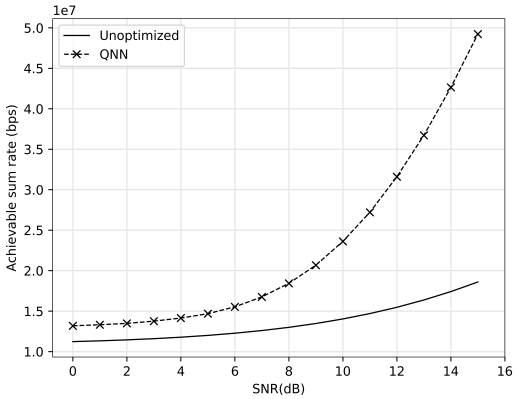

Fig. 4. The achievable sumrate.

4.3 Complexity Analysis

The complexity of QNN was analyzed as follows. First, pre-processing was conducted as described in Eq. (10), which utilized the $\mathbf{H}(\cdot)$ operation, resulting in $\mathcal{O}(1)$. Second, the feed-forward for QNN was described in Eq. (13). The weight encoding data utilized the $\mathbf{RY}\left(\tanh\left[\mathbf{u}_n\right]\right)$ operation, resulting in $\mathcal{O}(1)$. The connection between each qubit utilized the $\prod_{n=1}^{N_{\text{input}}} \mathbf{CZ}\left(|\mathbf{u}_n\rangle \,\middle|\, |\mathbf{u}_{n-1}\rangle\right)$ operation, resulting in $\mathcal{O}(N_{\text{input}})$. The input encoding data utilized $\mathbf{RX}\left(\tanh\left[w_n\right]\right)$ operation, resulting in $\mathcal{O}(1)$. Thus, the total complexity for $\mathbb{U}_{\text{QNN}} \in \mathcal{O}(1) + \mathcal{O}(N_{\text{input}}) + \mathcal{O}(1) \approx \mathcal{O}(N_{\text{input}})$. Finally, the overall complexity of QNN $\mathcal{O}(1) + \mathcal{O}(N_{\text{input}}) \approx \mathcal{O}(N_{\text{input}})$. On the other hand, based on [14], the complexity of a classical neural network can be defined as $\mathcal{O}((N_{\text{input}})^2)$. It can be concluded that the complexity of the QNN is lower than the classical neural network.

Ⅴ. Conclusions

This study proposed quantum neural network (QNN) optimization for joint optimization in MU MIMO-NOMA. Specifically, the QNN was applied to the joint optimization of precoders, combiners, and power allocation. The numerical results of MU MIMO-NOMA utilizing the proposed QNN have been presented. The results show that the proposed QNN outperformed the unoptimized scheme by achieving a higher achievable sum rate. The effects of employing different quantum circuit designs can be explored in the future

References

[1] O. Elijah, S. K. A. Rahim, W. K. New, C. Y. Leow, K. Cumanan, and T. K. Geok, "Intelligent massive mimo systems for beyond 5g networks: An overview and future trends," *IEEE Access*, vol. 10, pp. 102532-102563, 2022.

[2] D. d. S. Brilhante, J. C. Manjarres, R. Moreira, et al., "A literature survey on ai-aided beamforming and beam management for 5g and 6g systems," *Sensors*, vol. 23, no. 9, p. 4359, 2023.

[3] J. Zhang, X. Yu, and K. B. Letaief, "Hybrid beamforming for 5g and beyond millimeter-wave systems: A holistic view," *IEEE Open J. Commun. Soc.*, vol. 1, pp. 77-91, 2019.

[4] H. Hua, J. Xu, and T. X. Han, "Optimal transmit beamforming for integrated sensing and communication," *IEEE Trans. Veh. Technol.*, 2023.

[5] H. Al Kassir, Z. D. Zaharis, P. I. Lazaridis, N. V. Kantartzis, T. V. Yioultsis, and T. D. Xenos, "A review of the state of the art and future challenges of deep learning-based beamforming," *IEEE Access*, vol. 10, pp. 80869-80882, 2022.

[6] H. Hojatian, J. Nadal, J.-F. Frigon, and F. Leduc-Primeau, "Unsupervised deep learning for massive mimo hybrid beamforming," *IEEE Trans. Wireless Commun.*, vol. 20, no. 11, pp. 7086-7099, 2021.

[7] Y. Chen, X. Wen, and Z. Lu, "Achievable spectral efficiency of hybrid beamforming massive mimo systems with quantized phase shifters, channel non-reciprocity and estimation errors," *IEEE Access*, vol. 8, pp. 71304-71317, 2020.

[8] J. Kim, H. Lee, S.-E. Hong, and S.-H. Park, "Deep learning methods for universal miso beamforming," *IEEE Wireless Commun. Lett.*, vol. 9, no. 11, pp. 1894-1898, 2020.

[9] M. R. G. Aghdam, B. M. Tazehkand, and R. Abdolee, "Joint optimal power allocation and beamforming for mimo-noma in mmwave communications," *IEEE Wireless Commun. Lett.*, vol. 11, no. 5, pp. 938-941, 2022.

[10] M. A. Almasi, L. Jiang, H. Jafarkhani, and H. Mehrpouyan, "Joint beamwidth and power optimization in mmwave hybrid beamforming-noma systems," *IEEE Trans. Wireless Commun.*, vol. 20, no. 4, pp. 2442-2456, 2020.

[11] J. Zhu, Q. Li, Z. Liu, H. Chen, and H. V. Poor, "Enhanced user grouping and power allocation for hybrid mmwave mimo-noma systems," *IEEE Trans. Wireless Commun.*, vol. 21, no. 3, pp. 2034-2050, 2021.

[12] A. A. Badrudeen, C. Y. Leow, and S. Won, "Performance analysis of hybrid beamforming precoders for multiuser millimeter wave noma systems," *IEEE Trans. Veh. Technol.*, vol. 69, no. 8, pp. 8739-8752, 2020.

[13] S. Jerbi, L. J. Fiderer, H. Poulsen Nautrup, J. M. Kübler, H. J. Briegel, and V. Dunjko, "Quantum machine learning beyond kernel methods," *Nat. Commun.*, vol. 14, no. 1, p. 517, 2023.

[14] B. Narottama and S. Y. Shin, "Quantum neural networks for resource allocation in wireless communications," *IEEE Trans. Wireless Commun.*, vol. 21, no. 2, pp. 1103-1116, 2022.
(https://doi.org/10.1109/TWC.2021.3102139)

[15] B. N. Silvirianti and S. Y. Shin, "Layerwise quantum deep reinforcement learning for joint optimization of uav trajectory and resource

allocation," *IEEE Internet Things J.*, vol. 11, no. 1, pp. 430-443, 2024. (https://doi.org/10.1109/JIOT.2023.3285968)

[16] E. Björnson, M. Bengtsson, and B. Ottersten, "Optimal multiuser transmit beamforming: A difficult problem with a simple solution structure [lecture notes]," *IEEE Signal Process. Mag.*, vol. 31, no. 4, pp. 142-148, 2014. (https://doi.org/10.1109/MSP.014.2312183)

[17] P. Wang, J. Fang, L. Dai, and H. Li, "Joint transceiver and large intelligent surface design for massive mimo mmwave systems," *IEEE Trans. Wireless Commun.*, vol. 20, no. 2, pp. 1052-1064, Feb. 2021. (https://doi.org/10.1109/TWC.2020.3030570)

[18] D. Wierichs, J. Izaac, C. Wang, and C. Y.-Y. Lin, "General parameter-shift rules for quantum gradients," *Quantum*, vol. 6, p. 677, 2022.

[19] H. Abraham, "Qiskit: An open-source framework for quantum computing," 2019.

Lia Suci Waliani

Feb. 2022 : B.Eng. degree, School of Electrical Engineering, Telkom University, Bandung, Indonesia.

Aug. 2024 : M.Eng. degree, Dept. of IT Convergence, Kumoh National Institute of Technology, Gumi, South Korea.

<Research Interests> Quantum neural networks, multiple-input multiple-output (MIMO), non-orthogonal multiple access (NOMA), and error correction coding.

Soo Young Shin

Feb. 1999 : B.Eng. degree, School of Electrical and Electronic Engineering, Seoul National University.

Feb. 2001 : M.Eng. degree, School of Electrical, Seoul National University.

Feb. 2006 : Ph.D. degree, School of Electrical Engineering and Computer Science, Seoul National University.

July 2006-June 2007 : Post Doc. Researcher, School of Electrical Engineering, University of Washington, Seattle, USA.

2007-2010 : Senior Researcher, WiMAX Design Laboratory, Samsung Electronics, Suwon, South Korea.

Sept. 2010-Current : Professor, School of Electronic Engineering, Kumoh National Institute of Technology.

<Research Interest> 5G/ 6G wireless communications and networks, signal processing, the Internet of Things, mixed reality, and drone applications.